REGULAR ARTICLE

Polymer Journal

Synthesis and Photoluminescence Properties of Pyrene-Incorporated Organic-Inorganic Polymer Hybrids

By Kenta KOKADO,[1] Takeru IWAMURA,[2] and Yoshiki CHUJO[1,]*

Pyrene-incorporated organic-inorganic polymer hybrids were synthesized from methacryloyl monomers, tetramethoxysilane (TMOS) and pyrene *via* the *in situ* polymerization method. The photoluminescence properties of the incorporated pyrene chromophore were studied by using hybrids those were obtained by changing the ratio of inorganic moieties. As compared with organic polymers or a silica glass, the excimer emission of pyrene chromophore increased in the polymer hybrids. The excimer emission can be affected by changing the organic/inorganic ratio or the species of organic polymers. In the case of employing hydrophilic polymers, the excimer emission intensity of pyrene increased. Also, the excimer emission intensity of pyrene increased in the polymer hybrids having low organic polymer content. Furthermore, the sensitivity against oxygen of these excimer emissions in the polymer hybrids was found to be tuned by the organic/inorganic ratio in the polymer hybrids or the oxygen permeability of the organic polymers employed for hybridization.

KEY WORDS: Sol-Gel / Hybrid / Pyrene / Photoluminescence / Oxygen /

The organic-inorganic hybrid materials have received considerable interest in the past decade because of the expectation of developing various materials with the interesting properties resulted from incorporation of organic and inorganic constituents, and their homogeneities at the nano-meter scale.[1–5] In our group, we have synthesized organic-inorganic polymer hybrid materials by introducing many different kinds of organic polymers into the sol-gel reaction of alkoxysilanes.[3,4,6] Sol-gel reaction enables incorporating organic polymers or chromophores in the silica matrix due to the low reaction temperature.[7] To obtain the nano-level homogeneous polymer hybrid materials, we have to design proper intermolecular interactions between the organic polymer and the inorganic silica matrix.[8–16]

Considering the microenvironment of the polymer hybrid, it is expected that there are so many and dense intermolecular interactions between organic and inorganic moieties inside of the polymer hybrid materials. Thus the molecular environment of such a polymer hybrid is quite different from that of organic polymer films or inorganic silica glasses. An organic molecule incorporated in such an environment seems to exhibit an unique behavior compared to that doped in organic or inorganic matrices. A polymer hybrid as a novel matrix namely has many possibilities to produce an innovative material derived from the character of the polymer hybrid.

On the other hand, pyrene is a typical functional chromophore molecule forming excimer state.[17] There are numerous studies about the internal environments of organic polymers, micells or biomolecules by analyzing the excimer formation of pyrenes.[18–20] The emission properties of these chromophores in some solid matrices can be generally affected by various factors such as polarity and viscosity of the local environment and free volume distribution around the chromophores.[21–24] Thus chromophores such as pyrene would show an increasing photoluminescence property when incorporated in organic inorganic polymer hybrid.

Furthermore, it is well known that the excimer emission of pyrene molecules is quenched sensitively under the condition of oxygen presence.[25–27] Some applications based on this notable character have been reported in recent years. This property is greatly affected by the oxygen permeability of the matrix. By employing a polymer hybrid as a host of pyrene molecules, the hydrophilic/hydrophobic profiles of the matrices or the organic polymer species will be changed easily to control the assembly of pyrene molecules and the oxygen permeability of the polymer hybrid. In the present study, we report the photoluminescence properties and the oxygen-sensing applications of pyrene-incorporated organic-inorganic polymer hybrids.

EXPERIMENTAL

Reagents and Apparatus

Scanning electron microscopy (SEM) measurements were conducted using a JEOL SEM JSM-5600 system. ^{1}H NMR spectra (400 MHz) were recorded on a JEOL JNM-EX400 instrument. ^{1}H chemical shifts are reported in ppm (δ) relative to tetramethylsilane. Gel permeation chromatographic analysis was carried out on a TOSOH G3000HXI by using DMF (containing 10 m*M* LiBr) as an eluent after calibration with polystyrene standards. FT-IR spectra were obtained on a Perkin-Elmer 2000 spectrometer in KBr pellets. Photoluminescence spectra were recorded on a Perkin-Elmer LS50B luminescence spectrometer at room temperature. Thermogravimetric analysis (TGA) was performed using a TG/DTA6200 (SEIKO Instruments, Inc., Tokyo) with heating rate of 10 °C/

[1]Department of Polymer Chemistry, Graduate School of Engineering, Kyoto University, Katsura, Nishikyo-ku, Kyoto 615-8510, Japan
[2]Institute for Environmental Sciences, University of Shizuoka, 52-1 Yada, Suruga-ku, Shizuoka 422-8526, Japan
*To whom correspondence should be addressed (Tel: +81-75-383-2604, Fax: +81-75-383-2605, E-mail: chujo@chujo.synchem.kyoto-u.ac.jp).

 doi:10.1295/polymj.PJ2007221

min in air. Powder X-ray diffraction (XRD) patterns were taken by using CuKα radiation with a Rigaku MiniFlex. Nitrogen adsorption porosimetry was conducted with BEL Japan Inc. Methyl methacrylate (MMA), 2-hydroxyethyl methacrylate (HEMA) and ethyleneglycol dimethacrylate (EDMA) were distilled under reduced pressure and stored under argon. 2,2′-Azobis(isobutyronitrile) (AIBN) was recrystallized from methanol. Pyrene was purchased from Wako Pure Chemical Industries, Ltd. and recrystallized from benzene. The other solvents and reagents were used as supplied.

Copolymerization of HEMA and MMA[28]

HEMA (6.50 g, 49.95 mmol), MMA (5.00 g, 49.94 mmol) and AIBN (0.82 g, 4.99 mmol) were dissolved in a mixed solvent (100 mL) of MEK and *n*-PrOH (v/v, 7/3) under argon atmosphere. After 24 h at 60 °C, the reaction mixture was poured into diethyl ether and the precipitated polymer was dried *in vacuo*. The obtained poly(HEMA-*co*-MMA) was characterized by ^{1}H NMR and IR spectra. The unit ratio of the copolymer was calculated from ^{1}H NMR spectra (HEMA/MMA = 51/49). Yield: 90%, GPC (eluent: DMF containing LiBr 10 m*M*): M_n = 8600 (M_w/M_n = 3.50).

Preparation of the Polymer Hybrids from MMA and TMOS (Typical Procedure)

MMA (500 mg) and AIBN (41 mg, 0.05 equiv.) were dissolved in ethanol (20 mL) with TMOS (1.27 g), 0.1 *M* HCl aqueous solution (10 equiv. to alkoxysilane), and 0.6 mL of pyrene ethanol solution (12 m*M*). After being stirred at 60 °C for 24 h, the mixture was placed in a polypropylene vessel covered with a wiping paper and left in air at 60 °C for 10 d. The obtained polymer hybrid was dried *in vacuo* at 60 °C for 2 d.

Preparation of the Polymer Hybrids from HEMA, MMA and TMOS (Typical Procedure)

HEMA (280 mg), MMA (220 mg) and AIBN (36 mg, 0.05 equiv.) were dissolved in ethanol (20 mL) with TMOS (1.27 g), 0.1 *M* HCl aqueous solution (10 equiv. to alkoxysilane), and 0.6 mL of pyrene ethanol solution (12 m*M*). After being stirred at 60 °C for 24 h, the mixture was placed in a polypropylene vessel covered with a wiping paper and left in air at 60 °C for 10 d. The obtained polymer hybrid was dried *in vacuo* at 60 °C for 2 d.

Preparation of the Polymer Hybrids from HEMA, EDMA and TMOS

HEMA (86 mg), EDMA (14 mg, 10 mol % of the organic content) and AIBN (6 mg, 0.05 equiv.) were dissolved in ethanol (20 mL) with TMOS (2.30 g), 0.1 *M* HCl aqueous solution (10 equiv. to alkoxysilane), and 0.6 mL of pyrene ethanol solution (12 m*M*). After being stirred at 60 °C for 24 h, the mixture was placed in a polypropylene vessel covered with a wiping paper and left in air at 60 °C for 10 d. The obtained polymer hybrid was dried *in vacuo* at 60 °C for 2 d.

Measurements of Fluorescence Intensity of Polymer Hybrids

The polymer hybrids were placed into the fluorescence cell. It can be seen that fluorescence at excitation wavelength near 310 nm is relatively insensitive to oxygen, while fluorescence above 345 nm increases directly as a function of oxygen. The oxygen insensitive region allows the construction of a fluorescence ratio (fluorescence at sensitivity λ/fluorescence at insensitivity λ) which retains oxygen sensitivity but tends to correct for variations in excitation light intensity or chromophore concentration. Therefore, the fluorescence spectra were recorded at two excitation wavelengths, 345 nm and 310 nm and the ratio of the fluorescence intensities at 475 nm (345 nm/310 nm) was calculated. The oxygen proportions of the atmosphere were 0% (under argon), 21% (under dry air), and 100% (under oxygen), respectively.

Nitrogen Adsorption Porosimetry

By calcinating polymer hybrids at 600 °C for 24 h, porous silica materials were obtained. The samples were dried at 150 °C for 6 h at reduced pressure before porosimetry measurements. The surface area and pore volume were calculated by Brunauer-Emmet-Teller (BET) equation in the range of 0.05 to 0.30 (p/p_0) and the pore size distribution was estimated by a micropore analysis method, termed as MP method.

RESULTS AND DISCUSSION

PMMA/Silica Polymer Hybrids

As shown in Scheme 1 and Table I, the pyrene incorporated poly(methyl methacrylate) (PMMA)/silica polymer hybrids were synthesized by acid-catalyzed sol-gel reaction of tetramethoxysilane (TMOS) using 0.1 *M* HCl aqueous solution. The polymerization of methyl methacrylate (MMA) was carried out at the same time with the sol-gel reaction (This method is called *in situ* polymerization method in this study), since it is difficult to prepare PMMA/silica polymer hybrid by introducing preformed PMMA into a sol-gel reaction. This is a very useful method to synthesize homogeneous polymer hybrid with the organic polymers having poor affinity with a silica gel.[29] Except at the high organic content (org./inorg. = 9/1, Run 4), we could synthesize homogeneous polymer hybrids in a wide

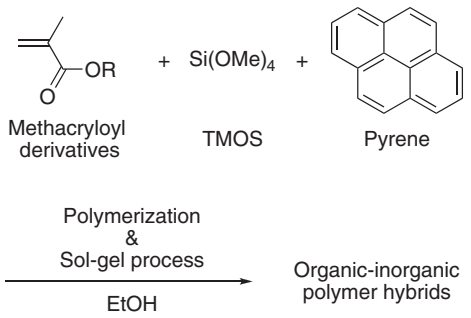

Scheme 1. Synthesis of polymer hybrids by *in situ* polymerization method.

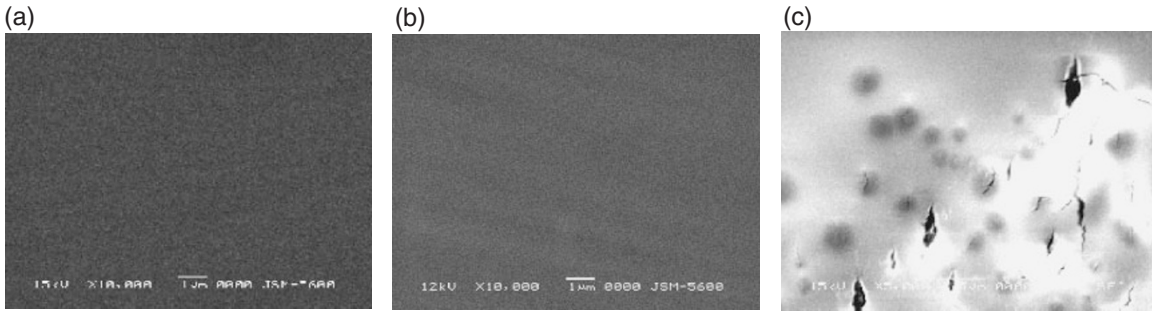

Figure 1. SEM images of PMMA/silica hybrids with organic/inorganic ratio of (a) 1/9 (Table I, Run 2), (b) 5/5 (Table I, Run 3), and (c) 9/1 (Table I, Run 4).

Table I. Synthesis of PMMA/silica polymer hybrids[a]

Run	MMA monomer (g)	TMOS (g)	Ceramic yield (%) Obsd.[b]	(Calcd.)	T_{d10}[b] (°C)	Appearance
1	0.000	2.528	—	(100.0)	—	transparent
2	0.104	2.277	89.3	(90.0)	619.1	transparent
3	0.500	1.267	47.1	(50.0)	293.0	transparent
4	0.903	0.258	—	(10.0)	—	turbid
5[c]	1.003	0.000	—	(0.0)	—	transparent

[a]Conditions: Organic monomer, AIBN (5 mol %) as a polymerization initiator, and pyrene (1.45 mg) were dissolved in 20 mL of EtOH with TMOS and 0.1 *M* HCl aq. (10 eq.) as a sol-gel catalyst. The mixture was sttired at 60 °C for 24 h, and the solvent was removed at 60 °C for 2 weeks. [b]Determined by TGA. [c]The monomer was dissolved in MEK/*n*-PrOH.

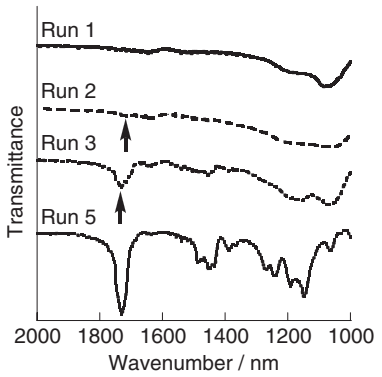

Figure 2. FT-IR spectra of PMMA/silica hybrids (Table I, Runs 1–3, and 5).

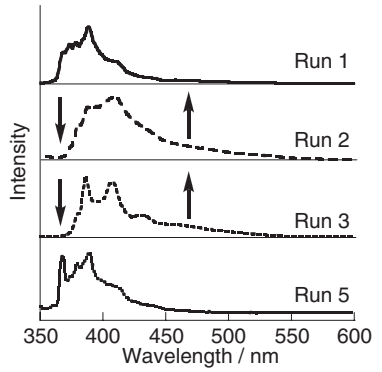

Figure 3. Photoluminescence spectra of PMMA/silica hybrids (Table I, Runs 1–3, and 5).

range of PMMA/silica ratio utilizing the *in situ* polymerization method. The calculated polymer contents were almost the same as the measured ones by thermogravimetric analysis (TGA) in air. This indicates that the *in situ* polymerization reaction proceeded almost ideally for the scheme. The phase of the obtained polymer hybrids was observed by XRD. In the XRD patterns of Runs 2 and 3 in Table I, broad amorphous halos ($2\theta = 20$–30°) were observed without any crystalline peaks. These results suggest that the polymer hybrids consist of amorphous silica gel and organic polymers.

The miscibility of organic and inorganic phase was confirmed by SEM. As shown in Figure 1, the phase separation between PMMA and silica was clearly observed in the sample with high organic contents (Run 4). In contrast, Runs 2 and 3 contained no microscopic or submicroscopic aggregations and separations consisting of organic or inorganic phase. From these results, it appeared that PMMA and silica were dispersed mutually at nano-meter level in the obtained hybrid materials.

FT-IR measurement of the obtained polymer hybrids was conducted to evaluate the intermolecular interaction between the organic polymers and the inorganic matrix (Figure 2). According to the previous studies, it is well known that the stretching vibration peak of carbonyl groups ($\nu_{C=O}$) derived from the organic polymer are shifted to lower wavenumbers region in polymer hybrid due to hydrogen bond formation between carbonyl groups and residual silanol groups.[3,30,31] In PMMA/silica polymer hybrids, $\nu_{C=O}$ was shifted to lower wavenumbers region apparently as the inorganic content increases. In Run 2, $\nu_{C=O}$ was shifted about 20 cm^{-1} compared to PMMA (1733 cm^{-1} to 1714 cm^{-1}). This result indicates that the hydrogen-bond is formed in the same manner in PMMA/silica system, which is considered to be responsible for the nano-meter level homogeneity of the dispersion-type hybrid materials.

The photoluminescence spectra of the obtained polymer hybrids are shown in Figure 3. The photoluminescence spectra of pyrene molecules in a silica glass (Run 1) or in a polymer film (Run 5) have strong emission around 375 nm, and there are no excimer emissions around 475 nm. In contrast, the emissions of polymer hybrids (Runs 2 and 3) have some contributions from the excimer region. In a pure silica matrix

Table II. Synthesis of P(HEMA-*co*-MMA)/silica polymer hybrids[a]

Run	HEMA monomer (g)	MMA monomer (g)	TMOS (g)	Ceramic yield (%) Obsd.[b]	(Calcd.)	T_{d10}[b] (°C)	Appearance
6	0.048	0.067	2.299	87.3	(90.0)	462.3	transparent
7	0.222	0.281	1.287	44.7	(50.0)	322.4	transparent
8[c]	0.444	0.577	0.000	—	(0.0)	—	transparent

[a]Conditions: Organic monomer, AIBN (5 mol %) as a polymerization initiator, and pyrene (1.45 mg) were dissolved in 20 mL of EtOH with TMOS and 0.1 *M* HCl aq. (10 eq.) as a sol-gel catalyst. The mixture was sttired at 60 °C for 24 h, and the solvent was removed at 60 °C for 2 weeks. [b]Determined by TGA. [c]The monomer was dissolved in MEK/*n*-PrOH.

(Run 1), since the absence of organic polymers as the hosts for pyrene molecules dispersed and immobilized them into the matrix, the diffusion-controlled excimer formation process was almost impossible.[32] On the other hand, pyrene molecules were dispersed homogeneously in a pure polymer film (Run 5) and stabilized due to their hydrophobic interactions, thus no excimer emission was observed. From this result, the polymer hybrids possess an outstanding environment for the pyrene molecules association to exhibit the excimer emissions.

The emission at 475 nm of Run 2 is stronger than that of Run 3, proposing that pyrene molecules aggregate more in the polymer hybrid including low organic content. It can be envisaged that, in the case of the polymer hybrid including low organic content (Run 2), where the pyrene molecules rarely associated with any organic moieties, the excimer formation would be almost impossible. However, the obtained data indicate the opposite results. Therefore, we can assume that the pyrene molecules are exclusively associated with the nanometer scale organic domain and that the overall volume fraction of the organic domain corresponds to the organic contents. As mentioned above, these polymer hybrids consist of numerous and dense intermolecular hydrogen-bonds between organic and inorganic components. Hydrophobic pyrene molecules should be dissociated from hydrophilic silica matrix or its hydrogen-bond interactions, and associate with the organic polymers *via* hydrophobic interactions, consequently the excimers formed. This hydrophobic interaction would be the driving force for pyrene molecules associations to form excimers because pyrene molecules were able to disperse into a pure silica matrix (Run 1). In the case of high organic contents (Run 3), since the total volume fraction of organic domain is also larger, pyrene molecules dispersed in the polymer hybrid broadly to exhibit monomer state emission with similar mannar as those in a pure polymer film (Run 5).

P(HEMA-*co*-MMA)/Silica Polymer Hybrids

For the reinforcement of the intermolecular hydrogen-bonds between organic and inorganic components, hydroxyethyl methacrylate (HEMA) as an organic monomer having hydrophilic functional group was employed to synthesize pyrene-incorporated polymer hybrids *via in situ* polymerization method as applied above (Table II). The samples in Runs 6–8 were optically transparent and contained no aggregations of organic or inorganic components from the SEM observation.

The photoluminescence spectra of the obtained polymer hybrids are shown in Figure 4. The pyrene excimer emissions

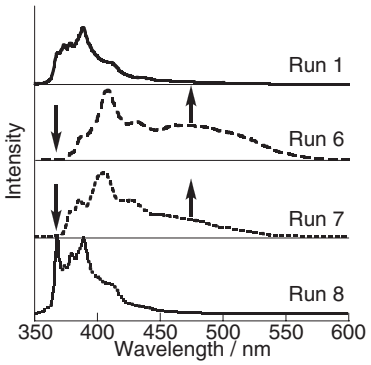

Figure 4. Photoluminescence spectra of P(HEMA-*co*-MMA)/silica hybrids (Table I, Run 1, and Table II, Runs 6–8).

around 475 nm were apparently increased in Run 6 and Run 7. Especially in Run 6, a peak was observed at 470 nm, indicating the tendency of pyrene excimer formation. These effects were attributed to change of the polymer species, *i.e.*, the reinforcement of the intermolecular hydrogen-bonds between organic and inorganic components. Since the volume fraction of hydrophilic interactions between organic and inorganic domains increased, and thus the volume fraction to accommodate pyrene molecules in it by hydrophobic interactions was diminished, pyrene molecules associated more effectively than the examples of PMMA/silica hybrids, while the sum of organic or inorganic components are same as above entries (Runs 2 and 3 respectively).

Nitrogen Adsorption Porosimetry

The homogeneity of these polymer hybrids was also confirmed by a nitrogen adsorption porosimetry method. The obtained polymer hybrids were calcinated to remove the organic components (Runs 3 and 7, organic/inorganic ratio of each polymer hybrid was 5/5.) by charring them at 600 °C for 24 h (Scheme 2). The siloxane network is so rigid that it would not be affected by the temperature. The previous studies justified that the pore size in the porous silica corresponds to the domain size of organic polymers in the original polymer hybrids.[16,31,33] For example, we reported the notable correlation between the pore size of polymer hybrids having the starburst dendrimer and the generation of the dendrimer employed.[31] Therefore, it is possible to verify the dispersity of organic polymers in the hybrids by measuring the pore size, pore volume, and the surface area.

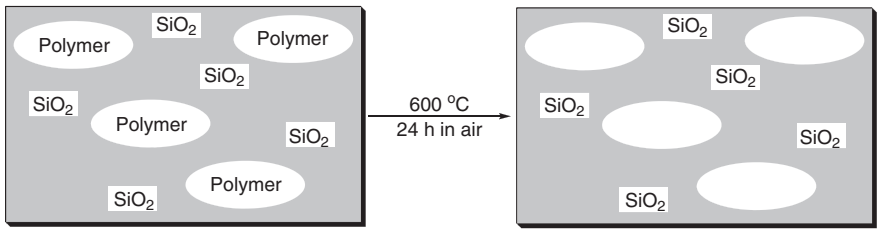

Scheme 2. Formation of porous silica from polymer hybrids by calcination.

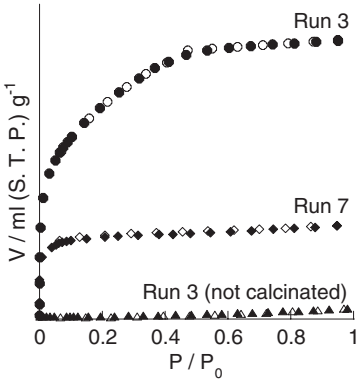

Figure 5. Adsorption isotherm curves of porous silica obtained from polymer hybrids.

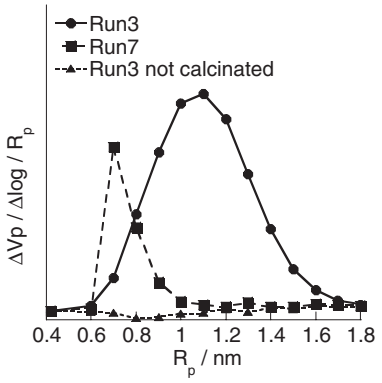

Figure 6. Pore size distribution plots of porous silica obtained from polymer hybrids (Runs 3 and 7).

Table III. Porosity of the obtained polymer hybrids[a]

Run	organic polymer	Pore volume[b] (cm^3/g)	Surface area[b] (m^2/g)	Pore diamieter[c] (nm)
3	PMMA	124	538	1.1
7	P(HEMA-*co*-MMA)	49	212	0.7
3[d]	PMMA	N/D	N/D	N/D

[a]The porous silica were odtained by charring the polymer hybrids at 600 °C for 24 h. [b]Calculated by the BET method. [c]Calculated by the MP method. [d]Not calcinated.

The porous silica prepared from Runs 3 and 7 showed a type I curve, indicating that the microporous silica was synthesized (Figure 5). The pore size, pore volume, and the surface area data are summarized in Table III. In Run 3 and Run 7, the volume of the adsorption of the nitrogen increased as increasing of the hydrophobicity of the organic polymer. In contrast, the volume of nitrogen was very little in case of Run 3 without calcinated posessing few pores. These results also indicate that the pores prepared by calcination of polymer hybrids were found to reflect the size of organic polymer domain in silica matrix. The surface area and volume of the porous silica were calculated by applying the BET method (Table III). The obtained porous silica had very large surface area and pore volume, especially in Run 3. Comparing Run 3 and Run 7, the pore volume and the surface area increased with increasing the hydrophobicity of the organic monomer.

Pore size distribution was calculated by a micropore analysis method, termed as MP method, from the desorption isotherm curve obtained by nitrogen absorption porosimetry of the porous silica to estimate the fineness of the pores. As can be seen in Figure 6, these samples (Run 3 and Run 7) had a nanometer scale silica pore, 1.1 nm, and 0.7 nm respectively, suggesting that the silica cage constructed during the sol-gel reaction was very small and allowed the polymer hybrid to have a molecular-level dispersion of the organic polymer inside the silica gel. The pore size of Run 7 (0.7 nm) was smaller about 0.4 nm than that of Run 3 (1.1 nm). Since the monomer of Run 7 is more hydrophilic than Run 3, and interacts with the silica cage more effectively, smaller pore would be formed. The exsistence of superfine pores in Run 7 should decrease the observed value of pore volume despite the quantity of employed organic polymers was almost same as that in Run 3. Considering the result of the porosimetry study, the organic domain size might be determined by the organic polymer species. P(HEMA-*co*-MMA) polymer chain should have a noticeable affinity with the silica matrix, whereas the PMMA polymer chain does not have enough affinity to disperse itself in a silica matrix homogeneously unless utilizing the *in situ* polymerization method. According to this study, changing the organic polymer species would considerably influence the silica morphology even though the synthesis method was same in each polymer hybrid.

Oxygen Quenching Properties

Pyrene excimer emission is well known to be quenched efficiently under existence of oxygen molecules due to its long excited lifetime (400 ns).[26,27] To examine the oxygen quenching properties of the polymer hybrids quantitatively, the ratio of emission intensities excited at 345 nm to 310 nm was adopted as a relative emission intensity.[34,35] The polymer

Table IV. Synthesis of organic-inorganic polymer hybrids for measuring oxygen quenching property of pyrene[a]

Run	organic monomer (g)	TMOS (g)	monomer/linker ratio (mol)	Ceramic yield (%) Obsd.[b]	(Calcd.)	T_{d10}[b] (°C)	Appearance
9	0.100 (HEMA)	2.299	0.9/0.1	87.4	90.0	457.5	transparent
2	0.104 (MMA)	1.287	1.0/0.0	89.3	90.0	619.1	transparent
3	0.500 (MMA)	0.000	1.0/0.0	47.1	50.0	293.0	transparent

[a]Conditions: Organic monomer, AIBN (5 mol %) as a polymerization initiator, and pyrene (1.45 mg) were dissolved in 20 mL of EtOH with TMOS and 0.1 *M* HCl aq. (10 eq.) as a sol-gel catalyst. The mixture was sttired at 60 °C for 24 h, and the solvent was removed at 60 °C for 2 weeks. [b]Determined by TGA.

hybrids for examination of oxygen quenching properties were prepared as expressed in Table IV. PMMA/silica polymer hybrids were used for Run 2 and Run 3 (Table IV) to examine an influence caused by the difference of organic/inorganic component ratio (1/9 and 5/5 respectively). And then in Run 9 in Table IV, a crosslinked PHEMA was employed as the organic component due to high oxygen permeability (PMMA $= 0.116 \times 10^{-13}$ cm^2/s·Pa, crosslinked PHEMA $= 5.43 \times 10^{-13}$ cm^2/s·Pa, respectively).[36] 1/9 organic/inorganic ratio was used for Run 9 to examine the effect of the oxygen permeability of the organic polymer. The organic component of Run 9, crosslinked PHEMA, was synthesized *via in situ* polymerization method as described in our previous paper by employing a crosslinking reagent, ethyleneglycol dimethacrylate (EDMA) in this case.[33,37]

Figure 7 shows the quenching of pyrene in polymer hybrids of different organic/inorganic ratio and organic polymers having different oxygen permeabilities by measuring the emission in atmospheres of argon, dry air and oxygen. Comparing Run 2 and Run 3, the pyrene emission of Run 3 had a more sensitivity than Run 2, indicating the organic/inorganic ratio, that is, the different oxygen permeability between PMMA and silica matrix, might concern with the oxygen sensitive emission properties. Furthermore, in Run 2 and Run 9, Run 9 apparently exhibited an excellent sensitivity against oxygen, whereas the organic/inorganic ratios of these two samples were the same. This suggests the possibility to tune the sensing of oxygen by changing the polymer species even in the case of very low organic polymer content.

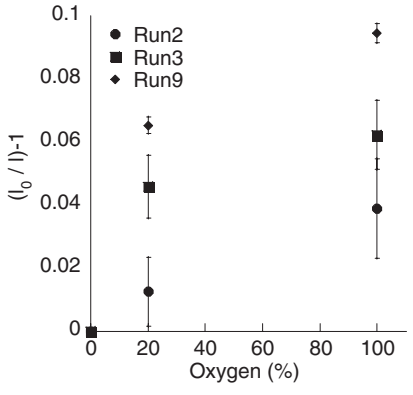

Figure 7. Oxygen quenching of pyrene in polymer hybrids of different polymer contents, or of different polymer species (Runs 2, 3, and 9).

CONCLUSION

As a summary, we were successful to obtain the pyrene-incorporated organic-inorganic polymer hybrids in a wide range of methacryloyl derivatives-silica ratio utilizing an *in situ* polymerization method. The obtained polymer hybrids could exhibit pyrene excimer photoluminescence effectively due to the modification of the internal environment of organic-inorganic polymer hybrids changed by organic polymer species or the synthesis method. The oxygen-sensitive photoluminescence of the obtained organic-inorganic polymer hybrids could be tuned by changing organic/inorganic ratio or oxygen permeability of the organic polymers. These characteristic properties could be usefully applied as various fields such as sensors and membranes.

Received: November 19, 2007
Accepted: December 24, 2007
Published: April 2, 2008

REFERENCES

1. H. Dislich, *J. Non-Cryst. Solids*, **73**, 599 (1985).
2. B. M. Novak, *Adv. Mater.*, **5**, 422 (1993).
3. Y. Chujo and T. Saegusa, *Adv. Polym. Sci.*, **100**, 11 (1992).
4. Y. Chujo and R. Tamaki, *MRS Bull.*, **26**, 389 (2001).
5. A. B. Descalzo, R. Martínez-Máñez, F. Sancenón, K. Hoffmann, and K. Rurack, *Angew. Chem. Int. Ed.*, **45**, 5924 (2006).
6. T. Ogoshi and Y. Chujo, *Compos. Interfaces*, **11**, 539 (2005).
7. C. J. Brinker and G. W. Scherer, "Sol-Gel Science The Physics and Chemistry of Sol-Gel Processing," Academic Press, Inc. San Diego, CA, 1990.
8. R. Tamaki, K. Samura, and Y. Chujo, *Chem. Commun.*, 1131 (1998).
9. R. Tamaki, S. Han, and Y. Chujo, *Silicon Chem.*, **1**, 409 (2002).
10. R. Tamaki and Y. Chujo, *Chem. Mater.*, **11**, 1719 (1999).
11. A. K. Achimuthu, K. Adachi, and Y. Chujo, *J. Polym. Sci., Part A: Polym. Chem.*, **42**, 785 (2004).
12. T. Iwamura, K. Adachi, and Y. Chujo, *Polym. J.*, **36**, 871 (2004).
13. K. Adachi, A. K. Achimuthu, and Y. Chujo, *Macromolecules*, **37**, 9793 (2004).
14. T. Ogoshi, H. Itoh, K. M. Kim, and Y. Chujo, *Macromolecules*, **35**, 334 (2002).
15. T. Ogoshi and Y. Chujo, *J. Polym. Sci., Part A: Polym. Chem.*, **43**, 3543 (2005).
16. T. Ogoshi and Y. Chujo, *Macromolecules*, **36**, 654 (2003).
17. F. M. Winnik, *Chem. Rev.*, **93**, 587 (1993).
18. I. Suzuki, M. Ui, and A. Yamauchi, *J. Am. Chem. Soc.*, **128**, 4498 (2006).
19. R. Humphry-Baker, M. Grätzel, and Y. Moroi, *Langmuir*, **22**, 11205 (2006).
20. R. B. Martin, L. Qu, Y. Lin, B. A. Harruff, C. E. Bunker, J. R. Gord,

L. F. Allard, and Y. P. Sun, *J. Phys. Chem. B*, **108**, 11447 (2004).
21. J. Matsui, M. Mitsushi, and T. Miyashita, *J. Phys. Chem. B*, **106**, 2468 (2002).
22. A. Campbell and P. Somasundran, *J. Colloid Interface Sci.*, **229**, 257 (2000).
23. M. Koussathana, P. Lianos, and G. Staikos, *Macromolecules*, **30**, 7798 (1997).
24. E. Stathatos, P. Lianos, U. L. Strangar, B. Orel, and P. judeinstein, *Langmuir*, **16**, 8672 (2000).
25. W. M. Vaughn and G. Weber, *Biochemistry*, **9**, 464 (1970).
26. W. Xu, R. Schmidt, M. Whaley, J. N. Demas, B. A. DeGraff, E. K. Karikari, and B. L. Farmer, *Anal. Chem.*, **67**, 3172 (1995).
27. B. J. Basu and K. S. Rajam, *Sens. Actuators B*, **99**, 459 (2004).
28. T. Iwamura, K. Adachi, and Y. Chujo, *Polym. Bull.*, **53**, 89 (2005).
29. R. Tamaki, K. Naka, and Y. Chujo, *Polym. Bull.*, **39**, 303 (1997).
30. Y. Chujo, E. Ihara, S. Kure, and T. Saegusa, *Macromolecules*, **26**, 5681 (1993).
31. Y. Chujo, H. Matsuki, S. Kure, T. Saegusa, and T. Yazawa, *J. Chem. Soc., Chem. Commun.*, 635 (1994).
32. T. Tani, *J. Ceram. Soc. Jpn.*, **21**, 111 (1986).
33. R. Tamaki and Y. Chujo, *J. Mater. Chem.*, **8**, 1113 (1998).
34. K. Tsujimoto, M. Semadeni, M. Huflejt, and L. Packer, *Biochem. Biophys. Res. Commun.*, **155**, 123 (1988).
35. M. Kates, N. Moldoveanu, and L. C. Stewart, *Biochim. Biophys. Acta*, **1169**, 46 (1993).
36. W. H. Yang, V. F. Smolen, and N. A. Peppas, *J. Membr. Sci.*, **9**, 53 (1981).
37. R. Tamaki, T. Horiguchi, and Y. Chujo, *Bull. Chem. Soc. Jpn.*, **71**, 2749 (1998).

